

# Short-Chain PEG Mixed Monolayer Protected Gold Clusters Increase Clearance and Red Blood Cell Counts

Carrie A. Simpson, Amanda C. Agrawal, Andrzej Balinski, Kellen M. Harkness, and David E. Cliffel\*

Department of Chemistry, Vanderbilt University, Nashville, Tennessee 37235-1822, United States

The use of gold nanoparticles (AuNP) for biological applications is a growing field in chemistry. Their small sizes (<5 nm) and the ability to functionalize their monolayer for specific applications make them excellent candidates for *in vivo* imaging,<sup>1,2</sup> targeting vesicles,<sup>3</sup> and peptide epitope presentation.<sup>4,5</sup> Much work has focused on the characterization and modification of water-soluble gold nanoparticles, functionalized primarily with glutathione and *N*-(2-mercaptopropionyl)glycine (tiopronin).<sup>6,7</sup> These water-soluble monolayer-protected clusters are ideal candidates for *in vivo* studies given both ligands are routinely used *in vivo* for medicinal purposes.<sup>8–10</sup>

Polyethylene glycol (PEG) has been shown to relieve nanotoxicity and allow the particles to escape the opsonization process.<sup>11–13</sup> The incorporation of PEG onto the surfaces of nanoparticles/rods has shown to significantly increase the residence half-life within the bloodstream.<sup>14–17</sup> Gref *et al.* showed the addition of PEG to a PLA nanoparticle significantly improved the circulation time *in vivo*,<sup>14</sup> while Feldheim and co-workers reported on the influence of PEG chain length and cellular internalization.<sup>18</sup> Their work showed stability increased with decreasing particle diameter and increasing PEG chain length. Other *in vitro* studies focused on PEG-ylated species in rat skin and intestine, showing smaller nanoparticles had a wider distribution.<sup>19</sup> While PEG-ylation provides immense benefits to *in vivo* applications of particles, previous reports have also shown the presence of an anti-PEG antibody in 25% of normal blood donors<sup>20,21</sup> as well as in response to injection with PEG-ylated polymer particles.<sup>22,23</sup> Therefore, if gold nanoparticles are to be used for *in vivo* applications, PEG must be incorporated into the monolayer at concentrations low enough to prevent an immune

**ABSTRACT** Monolayer-protected gold nanoparticles have great potential as novel building blocks for the design of new drugs and therapeutics based on the easy ability to multifunctionalize them for biological targeting and drug activity. In order to create nanoparticles that are biocompatible *in vivo*, polyethylene glycol functional groups have been added to many previous multifunctionalized particles to eliminate nonspecific binding. Recently, monolayer-protected gold nanoparticles with mercaptoglycine functionalities were shown to elicit deleterious effects on the kidney *in vivo* that were eliminated by incorporating a long-chain, mercapto-undecyl-tetraethylene glycol at very high loadings into a mixed monolayer. These long-chain PEGs induced an immune response to the particle presumably generating an anti-PEG antibody as seen in other long-chain PEG-ylated nanoparticles *in vivo*. In the present work, we explore the *in vivo* effects of high and low percent ratios of a shorter chain, mercapto-tetraethylene glycol within the monolayer using simple place-exchange reactions. The shorter chain PEG MPCs were expected to have better water solubility due to elimination of the alkyl chain, no toxicity, and long-term circulation *in vivo*. Shorter chain lengths at lower concentrations should not trigger the immune system to create an anti-PEG antibody. We found that a 10% molar exchange of this short-chain PEG within the monolayer met three of the desired goals: high water solubility, no toxicity, and no immune response as measured by white blood cell counts. However, none of the short-chain PEG mixed monolayer compositions enabled the nanoparticles to have a long circulation time within the blood as compared to mercapto-undecyl-ethylene glycol, which had a residence time of 4 weeks. We also compared the effects of a hydroxyl *versus* a carboxylic acid terminal functional group on the end of the PEG thiol on both clearance and immune response. The results indicate that short-chain-length PEGs, regardless of termini, increase clearance rates compared to the previous long-chain PEG studies, while carboxylated termini increase red blood cell counts at high loadings. Given these findings, short-chain, alcohol-terminated PEG, exchanged at 10%, was identified as a potential nanoparticle for further *in vivo* applications requiring short circulation lifetimes with desired features of no toxicity, no immune response, and high water solubility.

**KEYWORDS:** nanoparticle · TMPC · PEG-TMPC · murine study

response and to escape recognition by existing anti-PEG antibodies.

Successful synthesis of a biologically effective mixed monolayer particle is dependent upon the packing density of the PEG. Previous reports have shown the packing density of the PEG within the monolayer of the particle will influence the clearance time as well as the opsonization of the particle.<sup>14,24</sup> Two common terms to describe the packing

\* Address correspondence to d.cliffel@vanderbilt.edu.

Received for review November 19, 2010 and accepted April 7, 2011.

Published online April 07, 2011  
10.1021/nn103148x

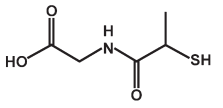
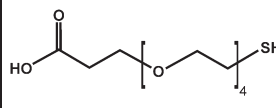
© 2011 American Chemical Society

of PEG on the particle's surface are (a) mushroom and (b) brush, where mushroom structures contain few PEG ligands in a disperse configuration relative to their positions on the monolayer and brush structures tightly pack the PEG into clusters on the surface.<sup>24</sup> Dispersivity of PEG may still allow for entry of opsonins between gaps in the monolayer, while brush structures' tight packing does not allow for fluid movement of the layer. It is this fluid movement that is believed to be the mechanism of opsonin repulsion; therefore, particle "overload" decreases the effectiveness of the PEG. For these reasons, a configuration between the two is predicted to be the optimum for biological efficiency *in vivo*. Exchange of ligands into the monolayer at various loadings has been performed previously by place-exchange reactions.<sup>25</sup> This process may be controlled stoichiometrically to produce a particle with a high or low percentage of a new thiol within the monolayer. While this has not been previously shown for PEG thiols, we expect place-exchange with PEG thiols to result in a brush/mushroom configuration.

Another consideration for PEG-ylated particle construction is charge. Prior *in vitro* studies by Stellacci and co-workers found that surface charge on the nanoparticle was responsible for cellular uptake, with the highest uptake being negatively charged particles (COOH), followed by positively charged (NH<sub>3</sub>), then neutrally charged particles (PEG).<sup>26</sup> A similar effect was observed by Reinhard and co-workers in their studies with large and small particles coated with both amines and carboxylic acids.<sup>27</sup> They observed two phenomena: (a) negatively charged particles increased the cellular uptake efficiency and (b) uncoated smaller particles also increased cellular uptake efficiency. Arvizo *et al.* examined the influence of charge on entry into the plasma membrane.<sup>28</sup> These studies suggest that charge is primarily responsible for the nanoparticles' interactions with living cells; however, there have not yet been any *in vivo* experiments that have tested this hypothesis.

We recently published research on the unexpected toxicity observed following the subcutaneous injection of tiopronin monolayer protected clusters (TMPC) in mice.<sup>29</sup> We eliminated this toxicity with the incorporation of a long-chain mercaptoundecyl-tetraethylene glycol (MUAPEG) into the monolayer at very high loadings. This mixed monolayer eliminated morbidity at all concentrations as well as alleviated all renal damage noted after injection with the original TMPC. In our previous report, we exchanged a 4:1 w/w ratio of MUAPEG:tiopronin, which, as noted by TGA, overloaded the particle, presumably producing a brush structure.<sup>29</sup> Herein, we describe the synthesis of two mixed monolayer particles, using both high and low percentages of a shorter chain mercapto-tetraethylene glycol (PEG<sub>4</sub>), presumably creating both a mushroom particle and a particle between the mushroom and

**TABLE 1. Ratios for PEG<sub>4</sub>-acid Place-Exchange Reactions (calculated tiopronin:PEG feed in solution) and Resulting PEG Surface Coverage Percentages by NMR and IM-MS<sup>a</sup>**

Tiopronin(Au): Free PEG Feed Ratio (mol:mol)	PEG Surface Coverage (mol percentage)	
	IM-MS	NMR
15:1	15%	10%
10:1	19%	13%
2:1	55%	60%
1:1	74%	75%
Tiopronin	Thiol-dPEG® 4-acid (PEG)	
		

<sup>a</sup> PEG feed ratio was determined from calculated molar concentrations of tiopronin on the monolayer surface as determined for original TMPCs.

brush configuration based on percentage PEG coverage as noted by both NMR and IM-MS. We then tested these nanoparticles *in vivo*. Our mixed monolayer consisted of tiopronin as the original ligand on the nanoparticles place-exchanged with one of two PEG<sub>4</sub> ligands. Both ligands consisted of a PEG<sub>4</sub> chain length but with different termini, a carboxylic acid (PEG<sub>4</sub>-acid) and an alcohol (PEG<sub>4</sub>-OH). While these PEG<sub>4</sub>'s were shorter (1.8 nm) than that used in our previous study (3.1 nm),<sup>29</sup> they are still considerably longer than tiopronin (0.7 nm). PEG is believed to produce its circulation benefits due to its ability to protract past the original tiopronin monolayer ligand, and this considerable 2.5-fold increase in ligand length should provide the needed shielding from opsonization for maximum circulation of the particle while reducing total antigenic PEG presentation to the immune system.

## RESULTS AND DISCUSSION

Table 1 shows the resulting percent PEG exchange after four separate place-exchange reactions of the PEG<sub>4</sub>-acid ligand by both NMR and IM-MS.

Both techniques for the analysis of surface coverage were not significantly different from each other in a paired Student's *t* test at the 95% confidence limit given a 1% surface coverage uncertainty in each measurement, and this similarity between the methods was noted previously.<sup>30</sup> Also shown is a positive correlation between concentration of PEG in solution and percent coverage; however, no significant gain in percent coverage was noted until larger PEG feed ratios were used. At lower feed ratios, the loading percentage difference between 10:1 and 15:1 was minimal. Therefore, for the *in vivo* experiments, only the 15:1 sample was used.

After confirmation of successful place-exchange reactions and sterilization with ethanol, the nanoparticles

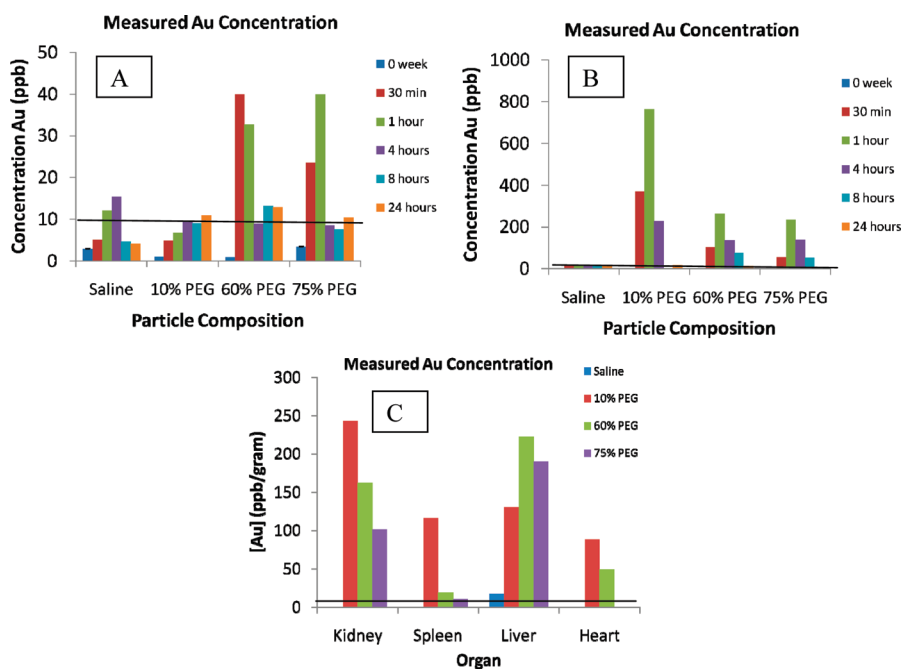


**Figure 1.** ICP-OES gold analysis for (a) blood, (b) urine, and (c) organs of PEG<sub>4</sub>-acid-injected mice 4 weeks postinjection. A 5  $\mu$ L sample was diluted in 10 mL of nitric acid/aqua regia solution (total dilution factor = 2000). Low concentrations of gold were noted in the bloodstream, while high concentrations were seen in the urine. No gold was observed at the 2- and 4-week time periods. Clearance profiles for the 10% group mimicked those previously seen for TMPCs. Gold analysis of the organs showed decreasing correlation of organ residence with increase in PEG percentage for both kidney and spleen. Black line signifies the detection limit of the ICP-OES at 10 ppb Au.

were injected subcutaneously as described in Simpson *et al.*<sup>29</sup> for *in vivo* experiments. Blood, urine, and organs (kidneys, heart, liver, and spleen) were monitored for gold content *via* inductively coupled plasma optical emission spectroscopy (ICP-OES). The results of the PEG<sub>4</sub>-acid 6-week study are shown in Figure 1.

The data clearly show the lower percentage PEG<sub>4</sub>-acid place-exchanged nanoparticles mimic the behavior of the TMPC,<sup>29</sup> producing low gold concentration in the bloodstream and high concentration in the urine in the first 24 h. The measured gold concentration in the blood and urine for all concentrations at 2 and 4 weeks was below the detection limit (5–10 ppb) of the ICP-OES and is not shown, suggesting the particle is cleared from the bloodstream primarily within the first 24 h. This is quite short; previous studies showed high concentrations of the long-chain MUAPEG nanoparticle at 2 and 4 weeks postinjection. It is also noted that the 10% place-exchange nanoparticle is the only one present in high quantity within all the organs studied, also characteristic of the TMPC. For the higher place-exchange loadings of PEG<sub>4</sub>-acid, gold concentrations comparable to those seen previously for long-chain alkyl PEG ligands were noted. Constant concentrations in both the blood and urine are present throughout the entire 24 h time period. A descending pattern, correlative with increasing PEG<sub>4</sub> percentage, is noted for residence within both the kidney and spleen. The 10% exchange particles show the highest residence within the kidney and spleen, mimicking that of TMPCs,

whereas the 60% and 75% exchanges show relatively no residence in the spleen and high residence in the liver, mimicking the behavior seen for MUAPEG-TMPCs. For the 75% exchange, the gold concentration in the heart was below the limit of detection of the ICP-OES. Given these findings, the 10% exchange provides the benefits of PEG-ylation with the targeting efficiency of the TMPC; however, the circulation time (24 h) is much shorter in comparison to that of previous studies with the MUAPEG ligand (4 weeks).<sup>29</sup> This provides evidence that the length of the chain may directly correlate with the circulation time of the nanoparticle.

To determine if the circulation was correlated to the terminus of the ligand, the experiment was repeated with a PEG<sub>4</sub>-OH. This ligand was chosen for two reasons: (1) our previous experiments showed a longer alkyl chain alcohol terminus elicited a relatively longer circulation time (4 weeks);<sup>29</sup> therefore, if the terminus influences circulation time, the alcohol terminus should lead to longer clearance; and (2) the chain lengths were exactly the same (4 PEG units); therefore, if the clearance time is the same as the carboxylic acid terminus, presumably the length of the chain may be responsible for the longer clearance time observed previously. The place-exchange reactions for the PEG<sub>4</sub>-OH ligand were conducted under the same optimized conditions. The feed ratios and percent PEG coverage by NMR may be found in the Supporting Information. The ICP-OES analysis of the 6-week study of the PEG<sub>4</sub>-OH ligand is shown in Figure 2.

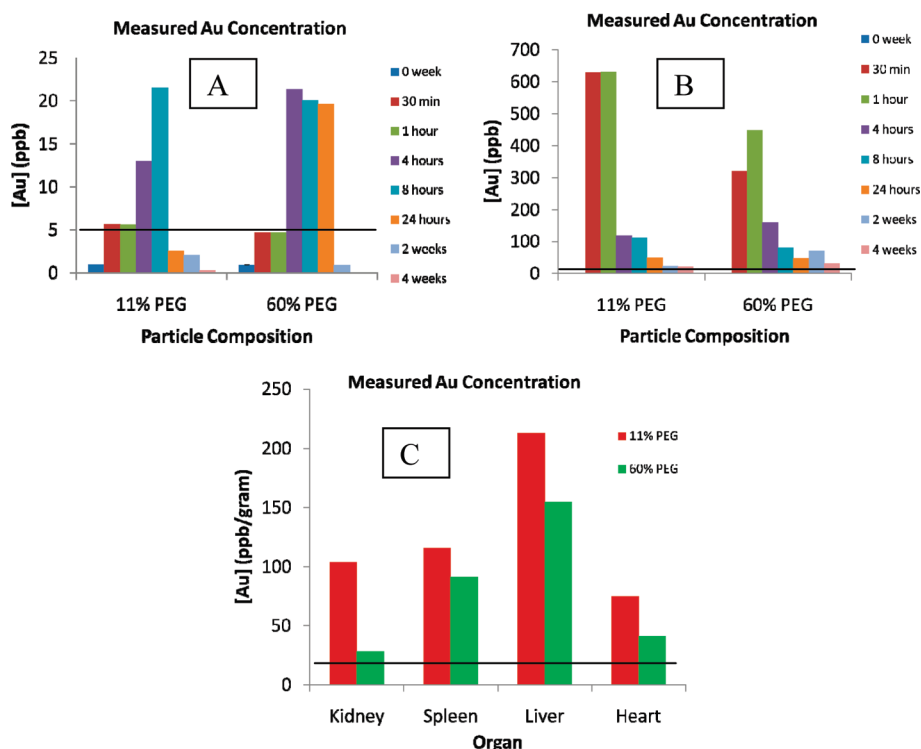


Figure 2. ICP-OES measured gold analysis for 5  $\mu\text{L}$  samples in 10 mL of nitric acid/aqua regia of (a) blood, (b) urine, and (c) organs of PEG<sub>4</sub>-OH-injected mice. Low concentrations of gold were noted in the bloodstream, while high concentrations were seen in the urine. Relatively no gold was observed at the 2- and 4-week time periods. Again, rapid clearance profiles were noted for both concentrations, signifying clearance is dependent on ligand length rather than end terminus. Gold analysis of the organs showed the largest accumulation of particles in the liver.

Given the correlation in the clearance times of the PEG<sub>4</sub>-acid and PEG<sub>4</sub>-OH, the PEG ligand terminus does not appear to affect the clearance rate or circulation time of the particle. It was also observed that the longer chain used previously does not seem to be necessary to prevent mortality, as all subjects used in both studies survived without any noticeable discomfort. Furthermore, the 10% percent PEG exchange provides both the benefits of PEG-ylation while retaining the original characteristics of the original monolayer, in this case tiopronin, making it the best choice for targeting. As final confirmation, both particle compositions were analyzed for both immune response and renal damage, as was noted in previous reports before selection of the best percent PEG exchange could be made.

Previous studies showed PEG-TMPCs elicited an increase white blood cell (WBC) count at 40  $\mu\text{M}$  using a MUAPEG alcohol terminus.<sup>29</sup> A perfect PEG-TMPC candidate for *in vivo* modeling should not only escape the opsonization process but also eliminate this immune response. Blood from all mice was analyzed by Coulter counter for WBC and red blood cell (RBC) counts to test for an immune response at 0, 2, and 4 weeks. The results are shown in Figure 3.

For PEG<sub>4</sub>-acid the 0  $\mu\text{M}$  shows no immune response as expected, nor does the 10% PEG exchange group. However, both the 60% and 75% exchange groups show significant change in RBC:WBC ratio (asterisked,

$p < 0.01$ ) after 4 weeks postinjection. This response is due to an increase in RBC count, not WBC count (Supporting Information). Therefore, no immune response is present. One of the few *in vivo* studies of PEG-ylated nanoparticles previously demonstrated that 50 to 250 nm polystyrene nanoparticles coated with alcohol-terminated PEGs were sequestered in the bone marrow and that this effect was enhanced as the particle size decreased.<sup>17</sup> No immune response was seen for either exchange of the PEG<sub>4</sub>-OH ligand. On the basis of these findings, the *in vivo* response seems to correlate with charged termini on short-chain ligands at high percent exchange, suggesting negative charge at high concentrations elicits higher RBC production. As shown in Alexis *et al.*,<sup>31</sup> hydroxyl particles present higher cellular uptake than carboxyl particles. This, in conjunction with observations made by Porter *et al.*<sup>32</sup> stating higher cellular uptake decreases the likelihood of distribution to the bone marrow, suggests the carboxyl terminus shifts the particles to the bone marrow, while hydroxyl terminus shifts the particles away from the bone marrow to the spleen and liver. It should also be noted that previous reports showed an immune response as measured by increased WBC counts from a MUAPEG with an OH terminus at high percent exchange.<sup>29</sup> Given these findings, the generation of an immune response *in vivo* is most likely dependent on nanoparticle concentrations rather than

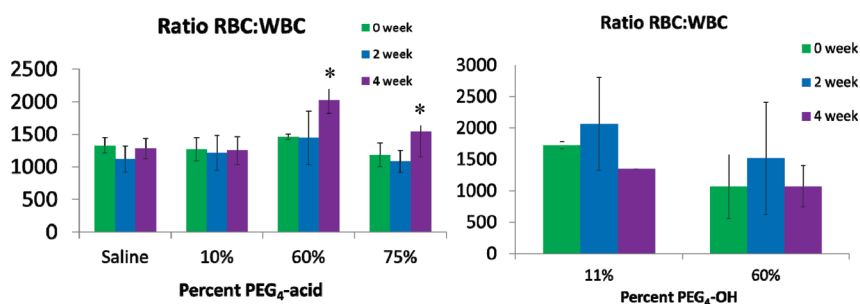


**Figure 3.** Coulter counter analysis of PEG<sub>4</sub>-acid (left) and PEG<sub>4</sub>-OH (right). No immune response was noted for the saline group or for the lowest percent exchange groups for either ligand. However, an immune response was noted for higher percent exchanges of PEG<sub>4</sub>-acid at 4 weeks, whereas no immune response was noted for PEG<sub>4</sub>-OH. This suggests higher percentages of PEG<sub>4</sub>-OH may be exchanged than PEG<sub>4</sub>-acid without triggering an immune response.

surface charge on the nanoparticle; however, the negative surface charge of the carboxylic acid terminus does induce an increase in RBC response at higher percent PEG<sub>4</sub>-acid exchanges.

Since no mortality was seen at any percent PEG exchange, the best synthetic route is a minimal amount of PEG-ylation to escape opsonization while also escaping an immune response. Therefore, a percent PEG exchange of approximately 10% of any ligand appears to meet all necessary criteria as the best candidate nanoparticle with further multifunctionalization for *in vivo* applications requiring short clearance times *in vivo*. As a final confirmation, histological examination was performed on all mice kidneys by Dr. Ken Salleng, DVM, Vanderbilt Division of Animal Care. Previous accounts showed extensive renal damage from TMPCs at 40  $\mu$ M without PEG-ylation, leading to death of all subjects.<sup>29</sup> Little to no renal damage was seen at 40  $\mu$ M with PEG-ylation, and no significant renal damage or toxicity was shown for any exchange ratio of PEGs used in this study. This combined with the 100% survival noted in all experimental subjects suggests that even small percentages of PEG-ylation provide the needed shielding from opsonization. Representative histological slides for the PEG<sub>4</sub>-acid may be found in the Supporting Information. These findings in conjunction with the immune response from Figure 3 suggest the 10% exchange ratio is the most desirable percent PEG exchange as a building block for epitope presentation projecting off the nanoparticle surface.<sup>5,33</sup> A recent paper<sup>34</sup> describes the use of neutron activation of gold nanoparticles to enable quantitative whole animal biodistribution studies, and this method, while

potentially more expensive, would enable a more quantitative approach to future studies for *in vivo* testing of potential therapeutic gold nanoparticles. This radiolabeling approach indicates that short-term (24 h) accumulation occurred mostly in the spleen and liver, consistent with our results in Figure 2C.

TMPCs have been shown to be toxic at high concentrations, which may be eliminated with PEG-ylation.<sup>29</sup> However, the amount of PEG-ylation must also be controlled if the TMPCs are to be used for long-term *in vivo* studies due to the presence of an immune response at high concentrations of PEG. We have shown that through simple place-exchange reactions, the amount of PEG-ylation on the TMPC may be controlled and a small percentage (10% coverage) is sufficient enough to prevent both mortality and presumably opsonization using short-chain PEGs, as no renal damage was noted in these studies. Furthermore, we have shown that the ligand end terminus plays no role in clearance or circulation time, and shorter chain ligands exhibit faster clearance rates than those previously studied. We have also shown that negatively charged ligands seem to increase RBC count at lower concentrations than neutral ligands. As a result of these findings and our previous study, we believe (a) the 10% exchange PEG-TMPC is an available candidate for future *in vivo* studies regardless of PEG ligand choice; (b) long-chain ligands are the best choice for long-circulation times; and (c) alcohol-terminated PEG thiols are more desirable for nanoparticle exchange than carboxylic acid termini due to lack of RBC increase at a wide range of percent coverage.

## EXPERIMENTAL SECTION

**Reagents.** Gold tetrachloroauric acid was synthesized in-house from 99.99% gold shot. Tetrachloroauric acid trihydrate was synthesized according to the literature<sup>35</sup> and stored in the freezer at  $-20$  °C. *N*-(2-Mercaptopropionyl)-glycine (tiopronin) (Sigma), Thiol-dPEG<sub>4</sub>-acid (Quanta Bio-design), Optima nitric acid (Fischer Scientific), methanol

(Fisher Scientific), acetic acid,  $\alpha$ -cyano-4-hydroxycinnamic acid (CHCA, Sigma-Aldrich), deuterium oxide, Zapoglobin (Beckman Coulter), and Isoton diluent (Beckman Coulter) were all used as received. Mercapto-PEG<sub>4</sub>-OH was synthesized based on a modification of previous literature methods that improved yield and reduced the number of synthetic steps.<sup>36</sup> Sterile phosphate-buffered saline was purchased

from Mediatech. A Millipore filtration system was used to obtain 18 M $\Omega$  water.

**Synthesis of TMPC.** TMPCs were synthesized by the traditional modified<sup>6</sup> Brust<sup>37</sup> reaction as prescribed in the literature. Briefly, to a 6:1 ratio (v/v) mixture of methanol and acetic acid was added tiopronin and tetrachloroauric acid trihydrate in a 3:1 (mol/mol) ratio (1.0 g HAuCl<sub>4</sub>/1.2 g tiopronin). The reaction was carried out at 0 °C and allowed to stir for ~30 min, whereupon the solution was removed under vacuum. The remaining black solid was dissolved in 100 mL of water and adjusted to pH 1 with hydrochloric acid. The solution was then loaded into cellulose ester dialysis membrane (MWCO = 10 000), placed in 4 L of water, and stirred continuously. The water was changed about every 12 h over a 1-week course. The solution was then removed under vacuum, and the resulting black nanoparticles were subsequently analyzed.

**Place-Exchange of PEG.** The tetra-EG chain was added to the TMPC *via* place-exchange reaction as described in Simpson *et al.*<sup>29</sup> with modifications. For the PEG<sub>4</sub>-acid experiments, 30 mg of TMPC was added to a 1.5 mg (15:1), 10 mg (2:1), or 20 mg (1:1) PEG sample in 3 mL of deionized water and allowed to stir for 1 h. The mixture was then loaded into cellulose ester dialysis membrane (MWCO = 10 000), placed in 4 L of deionized water, and stirred continuously to remove any excess PEG ligand within the solution. The water was changed *ca.* every 12 h over a 3-day course. The particles were then analyzed for purity by the same means as the original TMPCs. The PEG<sub>4</sub>-OH experiments were conducted under the same conditions with the following exceptions: 4 mg of TMPC was added to a 0.107 mg (15:1) and a 0.800 mg (2:1) PEG sample in 2 mL of deionized water and allowed to stir for 1 h.

**Nuclear Magnetic Resonance.** <sup>1</sup>H NMR spectra were collected of highly concentrated ligand and nanoparticle samples on a Bruker AC400 MHz NMR spectrometer in deuterium oxide (D<sub>2</sub>O). The tiopronin ligand spectrum was collected in DMSO-*d*<sub>6</sub> and CDCl<sub>3</sub> as previously reported.

**Ion Mobility-Mass Spectrometry.** *Sample Preparation.* In accordance with previous experiments,<sup>30</sup> place-exchanged AuNPs were dissolved in 10  $\mu$ L of deionized H<sub>2</sub>O and combined with 100  $\mu$ L of saturated CHCA and 1% NaCl in MeOH or up to 1:1 H<sub>2</sub>O/MeOH, depending on AuNP solubility. A 1  $\mu$ L portion of each was deposited on a stainless steel plate using the dried droplet method.<sup>38</sup> All MALDI-IM-MS analyses were performed using a Synapt HDMS (Waters Corp., Manchester, UK), equipped with a frequency-tripled Nd:YAG (355 nm) laser operated at a pulse repetition frequency of 200 Hz. All spectra were acquired in the positive ion mode.

*Peak Identification and Assignment.* Gold-containing ion signals were extracted and identified using the MassLynx 4.1 (Waters Corp.) software package. Identified peaks were checked against a list of possible ions for use in quantitation calculations. This list contained ions with Au<sub>4</sub>L<sub>4</sub> stoichiometries, potassium and sodium coordination, and methyl esterification. These modifications were included because of their preliminary observation in the ion mobility-mass spectra. This list was limited to Au<sub>4</sub>L<sub>4</sub> stoichiometries because, as mentioned in our recent report as a potential source of error, this particular ligand combination led to the presence of two sets of ions that differed by only 0.02 Da (−2 tiopronin, +1 PEG, +2 Na, and −1H), well within the limits of mass accuracy in this experiment.

*Data Processing for Quantitation.* In keeping with our previous experiments,<sup>30</sup> 1% relative abundance and 30 ppm mass accuracy cutoffs were used to reduce false positive identifications, and the monoisotopic ion abundances for the identified peaks were normalized to the expected monoisotopic abundance for each respective ion. The final set of identified peaks was used in quantitation calculations by the application of eq 1:

$$\left(\frac{X}{X+Y}\right)_{\text{AuNP}} = \frac{\sum C_{X,Y}(X)}{\sum C_{X,Y}(X+Y)} \quad (1)$$

For a nanoparticle with a binary ligand mixture, X and Y, the term on the left denotes the mole fraction of ligand X on the entire nanoparticle. On the right, the numerator is the sum of the multiples of the ion count (C<sub>X,Y</sub>) and the number of X ligands

present in each respective peak. The denominator is the sum of the multiples of the ion count (C<sub>X,Y</sub>) and the total number of ligands (X + Y) present in each respective peak. Together, these represent a mole fraction of the ligand X present on the nanoparticles.

**Thermogravimetric Analysis (TGA).** TGA was performed on all nanoparticle samples (*ca.* 5–10 mg) with a TGA 1000 instrument under N<sub>2</sub> flow (60 mL min<sup>−1</sup>), recording data from 25 to 800 °C at a heating rate of 20 °C min<sup>−1</sup>.

**Transmission Electron Microscopy.** The nanoparticles were prepared by adding ~1 mg of dried particle to 5 mL of 1 mM HCl solution and sonicating for ~20 min, and then they were dropped for slow evaporation onto ultrathin carbon grids (400 mesh, Ted Pella, Inc.). Images were obtained with a Phillips CM20T operating at 200 keV with a calibrated magnification of 414 kX. Results are reported as the mean  $\pm$  standard deviation obtained from the negatives using ImageJ software (NIH, <http://rsb.info.nih.gov/ij/>) using sample sizes of at least 50 particles from the TEM grid.

**Animal Models.** Animals were housed in a Vanderbilt Division of Animal Care (DAC) facility, fully certified by the Association for Assessment and Accreditation of Laboratory Animal Care (AALAC). Animals were housed under supervision of full-time veterinarians and staff, with an approved IACUC protocol. BALB/c/ANHsd mice, 5–6 week, female, weighing 15–16 g, were purchased from Harlan Laboratory. All animals were allowed 1 week for acclimation prior to experimentation. Nanoparticles were prepared in sterile phosphate-buffered saline (*n* = 5 mice/concentration group) and injected subcutaneously. Dosage concentrations were 40  $\mu$ M nanoparticles (8.19 mg for 15:1; 9.27 mg for 2:1; and 9.61 mg for 1:1, all dissolved in 3 mL of PBS) for PEG<sub>4</sub>-acid and (4.42 mg for 15:1 and 4.23 mg for 2:1, all dissolved in 1.5 mL of PBS) for PEG<sub>4</sub>-OH in a 200  $\mu$ L total volume of PBS. A 40  $\mu$ M concentration was chosen based upon results shown in Simpson *et al.*,<sup>29</sup> in which 40  $\mu$ M was the lowest concentration of MUAPEG particles shown to trigger an immune response. Blood was drawn *via* submandibular bleeding techniques, in compliance with our protocol and bleeding guidelines for mL/kg body weight per 2 weeks.<sup>39</sup> Urine was collected on cellophane with special precaution to avoid fecal contamination.<sup>40</sup> Four weeks postinjection, mice were euthanized *via* CO<sub>2</sub> asphyxiation, followed by cervical dislocation. Blood samples were divided among ICP-OES and Coulter counter, and organs were harvested for histology and trace metal analysis. Urine was tested for gold content.

**ICP-OES Analysis.** Fluid and tissue samples were prepared as described in Simpson *et al.*<sup>29</sup> with modifications. A 5  $\mu$ L sample size was chosen due to limitations in blood collection. A 5  $\mu$ L draw was consistently attained with all bleeds and, therefore, became our standard. Briefly, 5  $\mu$ L of blood or urine was diluted in 9 mL of 2% nitric acid (Optima grade, Fisher Scientific). Organs were excised, weighed, and dissolved in concentrated nitric acid (70% HNO<sub>3</sub>) and heated to dryness. The samples were then reconstituted in 9 mL of 2% nitric acid. After the 5  $\mu$ L fluid samples and organs were suspended in 9 mL of 2% nitric acid, a 1 mL aliquot of *aqua regia* (3:1 hydrochloric acid/nitric acid) was added to each sample. A 10 mL sample size was used in accordance with suggested ICP-OES guidelines. Samples were then loaded onto syringe filters to remove debris (0.2  $\mu$ m). Spectra were collected on a Perkin-Elmer ICP-OES Optima 700 DV. Argon plasma flow was set to 15 L min<sup>−1</sup>; nebulizer flow, at 0.2 L min<sup>−1</sup>. Pump flow was 1.5 mL min<sup>−1</sup> with rf power at 1300 W. Spectra were collected at the best gold intensity wavelength, 267.595 nm, with a delay time of 40 s for PEG<sub>4</sub>-acid and 30 s for PEG<sub>4</sub>-OH. Spectra were collected in triplicate and averaged for final gold content analysis.

**Coulter Counter Analysis of Blood.** Cell count analysis was performed on a Beckman Z1 Coulter particle counter. From whole blood samples, 40  $\mu$ L of blood was diluted into 20 mL of Isoton II diluent (Beckman Coulter) to create the WBC solution. Next, 200  $\mu$ L of WBC was transferred to 19.8 mL of diluent; this solution was used as prepared for the RBC counts. To the WBC solution was added 8 drops of Zap-Oglobin II lysing agent (Beckman Coulter). It was gently agitated and allowed to sit for 2 min, and then WBC counts were collected.

**Histology.** Organs were excised shortly after euthanasia, and sections of kidney were immediately fixed in formalin, 10% neutral buffered with 0.03% eosin (Sigma-Aldrich), and given to Vanderbilt Immuno Histology Core for H&E staining. The resulting slides were subsequently interpreted with help from Dr. Ken Salleng, DVM, Vanderbilt Division of Animal Care.

**Characterization of MPCs.** TMPCs were characterized using traditional analysis as documented in previous reports.<sup>6</sup> Figure S1 shows the NMR, TGA, and TEM for the TMPCs used in the PEG<sub>4</sub>-acid study, while Figure S2 shows the characterization data for the TMPCs used in the PEG<sub>4</sub>-OH study. NMR spectra show significant broadening, indicative of the presence of nanoparticles.<sup>41</sup> TGA analyses were within normal range for TMPCs, showing an organic loss of 38% for the PEG<sub>4</sub>-acid and 31% for the PEG<sub>4</sub>-OH. Final TEM analyses produced an average core diameter of  $2.5 \pm 0.6$  nm for the PEG<sub>4</sub>-acid and  $2.1 \pm 0.5$  nm for the PEG<sub>4</sub>-OH, both within the desired range as prescribed by Choi *et al.*<sup>11</sup> for optimum biological efficiency. This combined with the TGA analyses yielded estimated molecular formulas of Au<sub>485</sub>TiO<sub>182</sub> for the PEG<sub>4</sub>-acid and Au<sub>287</sub>TiO<sub>84</sub> for the PEG<sub>4</sub>-OH.

Figure S3 shows the NMR spectrum for the tiopronin ligand (blue), PEG<sub>4</sub>-acid ligand (red), and the 15:1 place-exchange of the PEG<sub>4</sub>-acid onto the TMPC (green). For quantification measurements, peaks must be identified that are uncommon to both ligands. For this study, the peak at 1.4 ppm for tiopronin (CH<sub>3</sub>) was compared to the peak at 2.5 ppm for the PEG<sub>4</sub>-acid ( $\alpha$ -CH<sub>2</sub> to carboxylic acid). The peak at 2.5 ppm in the tiopronin spectrum is attributed to the sulfur hydrogen, which is eliminated upon attachment to the gold core. The peak at 2.2 ppm is an artifact of the DMSO-*d*<sub>6</sub>. As is shown in the particle spectrum, both peaks are clearly visible and broad, making quantification fairly easy.

Figure S4 shows the NMR spectra for the three PEG<sub>4</sub>-acid exchange reactions used *in vivo* (15:1, 2:1, and 1:1). The intensity of the peak for tiopronin alone (1.6 ppm) decreases as the percentage of PEG<sub>4</sub>-acid applied to the monolayer increases. Quantification was performed as previously described<sup>30</sup> by integration of the PEG<sub>4</sub>-acid and tiopronin peaks. The result of the integration by NMR and the subsequent molecular formulas are shown in Figure S4 as well.

Figure S5 shows the NMR spectra for the PEG<sub>4</sub>-OH ligand and subsequent place-exchange reactions onto the TMPC. Integration of these peaks was performed differently, as there was no peak specifically isolated to the PEG ligand, as with the carboxylic acid terminus. Therefore, the peak located at approximately 3.8 ppm, which is attributable to both the PEG and tiopronin ligands, was used. Since the peak is attributable to both the CH<sub>2</sub> protons from both the tiopronin and PEG<sub>4</sub>-OH ligands, a simple mathematical calculation was performed to elicit the number of protons specific to the PEG ligand. From the CH<sub>3</sub> peak at 1.4 ppm (which is attributable to only tiopronin), we calculated how many CH<sub>2</sub> protons were attributable to tiopronin. We then subtracted this number from the integration at 3.8 ppm, leaving only the integration attributable to the PEG CH<sub>2</sub> protons. We then applied the same integration principles as with the PEG<sub>4</sub>-acid, using the same tiopronin peak at 1.4 ppm.

**Acknowledgment.** We would like to thank Dr. Ken Salleng, DVM, for his help with the mouse histology, the Vanderbilt Institute for Nanoscale Science and Engineering, and Whitney B. Ridenour and Richard M. Caprioli (Vanderbilt University Medical Center) for the use of the Synapt HDMS, which is supported by the VU Mass Spectrometry Research Core. This work was made possible by a grant from the National Institutes of Health, GM 076479.

**Supporting Information Available:** Full nanoparticle characterization and experimental methods are available free of charge via the Internet at <http://pubs.acs.org>.

## REFERENCES AND NOTES

- Hainfeld, J. F.; Slatkin, D. N.; Focella, T. M.; Smilowitz, H. M. Gold Nanoparticles: A New X-Ray Contrast Agent. *Br. J. Radiol.* **2006**, *79*, 248–253.

- Hainfeld, J. F.; Slatkin, D. N.; Smilowitz, H. M. The Use of Gold Nanoparticles to Enhance Radiotherapy in Mice. *Phys. Med. Biol.* **2004**, *49*, 309–315.
- Tkachenko, A. G.; Xie, H.; Coleman, D.; Glomm, W.; Ryan, J.; Anderson, M. F.; Franzen, S.; Feldheim, D. L. Multifunctional Gold Nanoparticle-Peptide Complexes for Nuclear Targeting. *J. Am. Chem. Soc.* **2003**, *125*, 4700–4701.
- Gerdon, A. E.; Wright, D. W.; Cliffl, D. E. Quartz Crystal Microbalance Detection of Glutathione-Protected Nanoclusters Using Antibody Recognition. *Anal. Chem.* **2005**, *77*, 304–310.
- Gerdon, A. E.; Wright, D. W.; Cliffl, D. E. Hemagglutinin Linear Epitope Presentation on Monolayer-Protected Clusters Elicits Strong Antibody Binding. *Biomacromolecules* **2005**, *6*, 3419–3424.
- Templeton, A. C.; Chen, S.; Gross, S. M.; Murray, R. W. Water-Soluble, Isolable Gold Clusters Protected by Tiopronin and Coenzyme a Monolayers. *Langmuir* **1999**, *15*, 66–76.
- Templeton, A. C.; Wuelfing, W. P.; Murray, R. W. Monolayer-Protected Cluster Molecules. *Acc. Chem. Res.* **2000**, *33*, 27–36.
- Farrell, N., Metal Complexes in Arthritis. In *Transition Metal Complexes as Drugs and Chemotherapeutic Agents*, 1st ed.; Kluwer Academic Publishing: Boston, 1989; pp 243–256.
- Herold, D. M.; Das, I. J.; Stobbe, C. C.; Iyer, R. V.; Chapman, J. D. Gold Microspheres: A Selective Technique for Producing Biologically Effective Dose Enhancement. *Int. J. Radiat. Biol.* **2000**, *76*, 1357–1364.
- Gillet, P.; Gavriloff, C.; Hercelin, B.; Salles, M. F.; Nicolas, A.; Netter, P. Pharmacokinetics of Tiopronin after Repeated Oral Administration in Rheumatoid Arthritis. *Fundam. Clin. Pharmacol.* **1995**, *9*, 205–206.
- Choi, H. S.; Liu, W.; Misra, P.; Tanaka, E.; Zimmer, J. P.; Ipe, B. I.; Bawendi, M. G.; Fangioni, J. V. Renal Clearance of Quantum Dots. *Nat. Biotechnol.* **2007**, *25*, 1165–1170.
- Niidome, T.; Yamagata, M.; Okamoto, Y.; Akiyama, Y.; Takahashi, H.; Kawano, T.; Katayama, Y.; Niidome, Y. PEG-Modified Gold Nanorods with a Stealth Character for *In Vivo* Applications. *J. Controlled Release* **2006**, *114*, 343–347.
- Hutter, E.; Boridy, S.; Labrecque, S.; Lalancette-Hebert, M.; Kriz, J.; Winnik, F. M.; Maysinger, D. Microglial Response to Gold Nanoparticles. *ACS Nano* **2010**, *4*, 2595–2606.
- Gref, R.; Domb, A.; Quellec, P.; Blunk, T.; Muller, R. H.; Verbavatz, J. M.; Langer, R. The Controlled Intravenous Delivery of Drugs Using PEG-Coated Sterically Stabilized Nanospheres. *Adv. Drug Delivery Rev.* **1995**, *16*, 215–233.
- Gref, R.; Luck, M.; Quellec, P.; Marchand, M.; Dellacherie, E.; Harnisch, S.; Blunk, T.; Muller, R. H. 'Stealth' Corona-Core Nanoparticles Surface Modified by Polyethylene Glycol (PEG): Influences of the Corona (PEG Chain Length and Density) and of the Core Composition on Phagocytic Uptake and Plasma Protein Absorption. *Colloids Surf., B* **2000**, *18*, 301–313.
- Moghimi, S. M.; Hunter, A. C.; Murray, J. C. Long-Circulating and Target-Specific Nanoparticles: Theory to Practice. *Pharmacol. Rev.* **2001**, *53*, 283–318.
- Moghimi, S. M.; Porter, C. J. H.; Muir, I. S.; Illum, L.; Davis, S. S. Non-Phagocytic Uptake of Intravenously Injected Microspheres in Rat Spleen: Influence of Particle Size and Hydrophilic Coating. *Biochem. Biophys. Res. Commun.* **1991**, *177*, 861–866.
- Liu, Y.; Shipton, M. K.; Ryan, J.; Kaufman, E. D.; Franzen, S.; Feldheim, D. L. Synthesis, Stability, and Cellular Internalization of Gold Nanoparticles Containing Mixed Peptide-Poly(Ethylene Glycol) Monolayers. *Anal. Chem.* **2007**, *79*, 2221–2229.
- Sonavane, G.; Tomoda, K.; Sano, A.; Ohshima, H.; Terada, H.; Makino, K. In Vitro Permeation of Gold Nanoparticles through Rat Skin and Rat Intestine: Effect of Particle Size. *Colloids Surf. B. Biointerfaces* **2008**, *65*, 1–10.
- Armstrong, J. K.; Leger, R.; Wenby, R. B.; Meiselman, H. J.; Garratty, G.; Fisher, T. C. Occurrence of an Antibody to Poly(Ethylene Glycol) in Normal Donors. *Blood* **2003**, *102*, 556A.

21. Leger, R. M.; Arndt, P.; Garratty, G.; Armstrong, J. K.; Meiselman, H. J.; Fisher, T. C. Normal Donor Sera Can Contain Antibodies to Polyethylene Glycol (PEG). *Transfusion* **2001**, *41*, 29S.
22. Armstrong, J. K.; Hempel, G.; Koling, S.; Chan, L. S.; Fisher, T. C.; Meiselman, H. J.; Garratty, G. Antibody against Poly-(Ethylene Glycol) Adversely Affects PEG-Asparaginase Therapy in Acute Lymphoblastic Leukemia Patients. *Cancer* **2007**, *110*, 103–111.
23. Richter, A. W.; Akerblom, E. Antibodies against Polyethylene Glycol Produced in Animals by Immunization with Monomethoxy Polyethylene Glycol Modified Proteins. *Int. Arch. Allergy Appl. Immunol.* **1983**, *70*, 124–131.
24. Owens, D. E.; Peppas, N. A. Opsonization, Biodistribution, and Pharmacokinetics of Polymeric Nanoparticles. *Int. J. Pharm.* **2006**, *307*, 93–102.
25. Hostetler, M. J.; Templeton, A. C.; Murray, R. W. Dynamics of Place-Exchange Reactions on Monolayer-Protected Gold Cluster Molecules. *Langmuir* **1999**, *15*, 3782–3789.
26. Verma, A.; Stellacci, F. Effect of Surface Properties on Nanoparticle-Cell Interactions. *Small* **2010**, *6*, 12–21.
27. Thubagere, A.; Reinhard, B. M. Nanoparticle-Induced Apoptosis Propagates through Hydrogen-Peroxide-Mediated Bystander Killing: Insights from a Human Intestinal Epithelium *in Vitro* Model. *ACS Nano* **2010**, *4*, 3611–3622.
28. Arvizo, R.; Miranda, O.; Thompson, M.; Pabelick, C.; Bhattacharya, R.; Robertson, J.; Rotello, V.; Prakash, Y.; Mukherjee, P. Effect of Nanoparticle Surface Charge at the Plasma Membrane and Beyond. *Nano Lett.* **2010**, *10*, 2543–2548.
29. Simpson, C. A.; Huffman, B. J.; Gerdon, A. E.; Cliffel, D. E. Unexpected Toxicity of Monolayer Protected Gold Clusters Eliminated by PEG-Thiol Place-Exchange Reactions. *Chem. Res. Toxicol.* **2010**, *23*, 1608–1616.
30. Harkness, K. M.; Hixson, B. C.; Fenn, L. S.; Turner, B. N.; Rape, A. C.; Simpson, C. A.; Huffman, B. J.; McLean, J. A.; Cliffel, D. E. A Structural Mass Spectrometry Strategy for the Relative Quantitation of Ligands on Mixed Monolayer-Protected Gold Nanoparticles. *Anal. Chem.* **2010**, *82*, 9268–9274.
31. Alexis, F.; Pridgen, E.; Molnar, L. K.; Farokhzad, O. C. Factors Affecting the Clearance and Biodistribution of Polymeric Nanoparticles. *Mol. Pharmaceutics* **2008**, *5*, 505–515.
32. Porter, C. J. H.; Moghimi, S. M.; Illum, L.; Davis, S. S. The Polyoxyethylene/Polyoxypropylene Block Co-Polymer Poloxamer-407 Selectively Redirects Intravenously Injected Microspheres to Sinusoidal Endothelial Cells of Rabbit Bone Marrow. *FEBS Lett.* **1992**, *305*, 62–66.
33. Gerdon, A. E.; Wright, D. W.; Cliffel, D. E. Epitope Mapping of the Protective Antigen of *B. anthracis* by Using Nanoclusters Presenting Conformational Peptide Epitopes. *Angew. Chem., Int. Ed.* **2006**, *45*, 594–598.
34. Lipka, J.; Semmler-Behnke, M.; Sperling, R. A.; Wenk, A.; Takenaka, S.; Schleh, C.; Kissel, T.; Parak, W. J.; Kreyling, W. G. Biodistribution of PEG-Modified Gold Nanoparticles Following Intratracheal Instillation and Intravenous Injection. *Biomaterials* **2010**, *31*, 6574–6581.
35. Brauer, G. *Handbook of Preparative Inorganic Chemistry*, 1st ed.; Academic Press: New York, 1965; p 1054.
36. Balinski, A. Masters Thesis, Vanderbilt University, Nashville, 2010.
37. Brust, M.; Fink, J.; Bethel, D.; Shiffrin, D. J.; Whyman, R. Synthesis of Thiol-Derivatized Gold Nanoparticles in a Two-Phase Liquid-Liquid System. *J. Chem. Soc., Chem. Commun.* **1994**, 801.
38. Karas, M.; Hillenkamp, F. Laser Desorption Ionization of Proteins with Molecular Masses Exceeding 10,000 Da. *Anal. Chem.* **1988**, *60*, 2299–2301.
39. NIH. Guidelines for Survival Bleeding of Mice and Rats. *Periodical* [Online], 2005 (accessed 05/2008).
40. Kurien, B. T.; Scofield, R. H. Mouse Urine Collection Using Clear Plastic Wrap. *Lab. Anim.* **1998**, *33*, 83–86.
41. Kohlman, O.; Steinmetz, W. E.; Mao, X.-A.; Wuelfing, W. P.; Templeton, A. C.; Murray, R. W.; Johnson, C. S. NMR Diffusion, Relaxation, and Spectroscopic Studies of Water Soluble, Monolayer-Protected Gold Nanoclusters. *J. Phys. Chem. B* **2001**, *105*, 8801–8809.